

The Role of Ventilation
15th AIVC Conference, Buxton, Great Britain
27-30 September 1994

**Measurement and Modelling of Aerosol
Particle Flow in an Environmental Chamber**

N Adam, K W Cheong, S B Riffat, L Shao

Building Technology Group, School of Architecture,
University of Nottingham, NG7 2RD United Kingdom

SYNOPSIS

This paper is concerned with measurement of air and aerosol particle exchange efficiency in a single zone chamber. Aerosol particles and tracer gases were injected into the chamber and their concentrations were monitored as a function of time. The chamber was provided with supply and exhaust terminals which allowed various airflow and particle patterns (e.g. piston flow, displacement flow) to be investigated. The effect of airflow pattern on deposition rate of aerosol particles on the surfaces of the chamber was determined. This paper also describes the application of computational fluid dynamics (CFD) modelling for the prediction of particle flow in the chamber. The CFD model, FLUENT, was used for this investigation and results were compared with particle and tracer-gas measurements.

LIST OF SYMBOLS

a_1, a_2, a_3	constants
A	surface area of chamber, (m^2)
C_D	drag coefficient
d	diameter of particle, (μm)
F_D	drag force, (N)
F_X	force acting on a particle due to virtual mass and pressure gradient in a fluid, (N)
I	tracer-gas exchange rate, ($\mu g/m^3h$ or h^{-1})
P	particle-exchange rate, ($\mu g/m^3h$ or h^{-1})
Re	relative Reynolds number
t	time, (s)
u	component of velocity in the x direction, (m/s)
V	velocity, (m/s)
V_Z	volume of zone, (m^3)
α	particle deposition rate, ($\mu g/m^2h$)
η_a	average air exchange efficiency
η_p	average particle exchange efficiency
ρ	density, (kg/m^3)
τ_{TE}	age of air at the exhaust terminal, (min)
τ_{Ti}	age of air at point i in the chamber, (min)
τ_{PE}	age of particle at the exhaust terminal, (min)
τ_{Pp}	age of particle at point p in the chamber, (min)
μ	molecular viscosity of air, (kg/ms)
∞	local air
p	particle

1. INTRODUCTION

Particulate pollutants in buildings can have damaging effects on the health of occupants. Studies have shown that indoor aerosol particles influence the incidence of sick building syndrome [1]. Some airborne particles are associated with allergies because they transport viruses and bacteria. Particulate pollutants can be transported between zones; this can have serious effects in hospitals and buildings used by the micro-electronic and pharmaceutical industries [2]. Deposition of airborne particles in museums and galleries may lead to perceptible soiling within a short period and ultimately result in damage to works of art [3].

The concentration of indoor aerosol particles can be reduced by using different ventilation strategies such as displacement and perfect mixing. However, there are insufficient data to quantify the effectiveness of these methods, as removal of particles is influenced by particle deposition rate, particle type, sizes, sources and concentrations.

This work aims to study various ways of removing aerosol particles from a mechanically-ventilated room and determine the effectiveness of each technique. This study also looks at the distribution of particles at four different locations in the chamber. Computational fluid dynamics (CFD) was also used to model the particle movement.

2. EXPERIMENTAL WORK

Measurements were carried out in a tightly-sealed chamber (3m x 2.5m x 2.4m) as shown in Figure 1. A variable-speed axial fan supplies fresh air to the chamber via a 0.3m diameter ductwork and 2m x 0.5m diffusers. Air is removed from the chamber via three diffusers which allows different ventilation strategies (shown in Figure 2) to be examined. The chamber was used for measurement of air exchange efficiency and particle exchange efficiency.

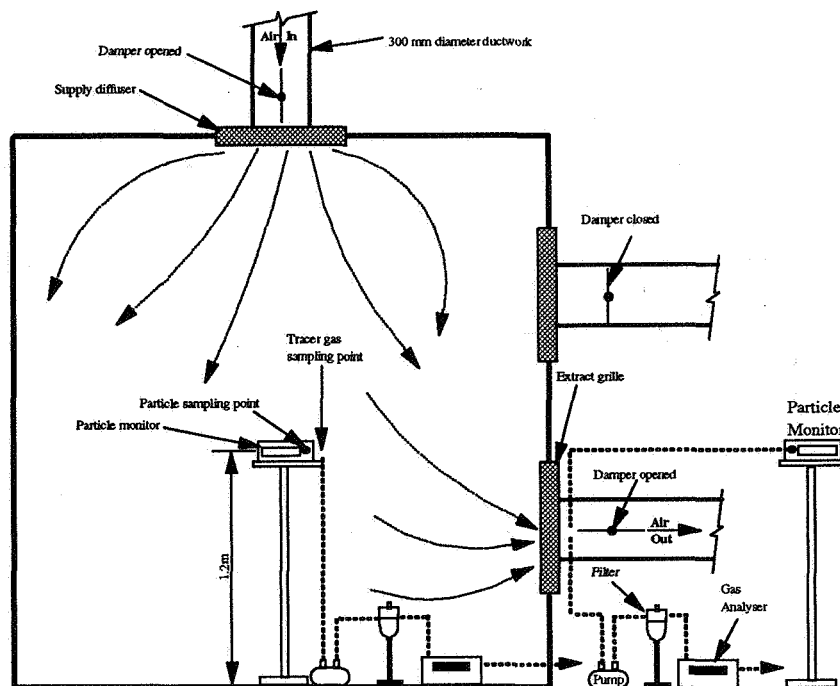


Figure 1 Schematic of the chamber and instrumentation

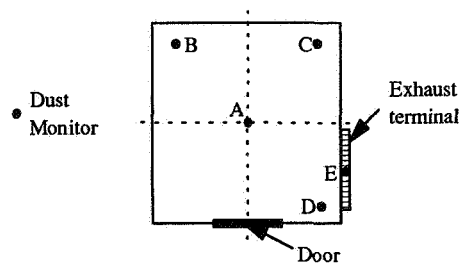


Figure 1a Location of dust monitors in environmental chamber, (Plan)

The experimental procedure involved injecting SF₆ tracer-gas and oil-smoke particles into the chamber with all dampers shut and all fans off. A desk fan was used to assist mixing. After a mixing period of 10 minutes, the desk fan was switched off. Once a uniform concentration of tracer-gas and smoke particles was achieved in the chamber, dampers at respective diffusers were opened and the axial fans were switched on. At the same time, simultaneous monitoring of the concentration of tracer-gas and smoke particles ($0.5 \mu\text{m} < d < 2 \mu\text{m}$) commenced at the exhaust terminal, in the centre of the chamber and three other locations (see Figure 1a). An infra-red gas analyser type BINOS 1000 made by Rosemount Ltd., U.K. and an infra-red particle monitor type Grimm 1.100 manufactured by Grimm Ltd., Germany were used to monitor the concentrations of tracer-gas and particles, respectively. A series of five different airflow rates was used for each condition.

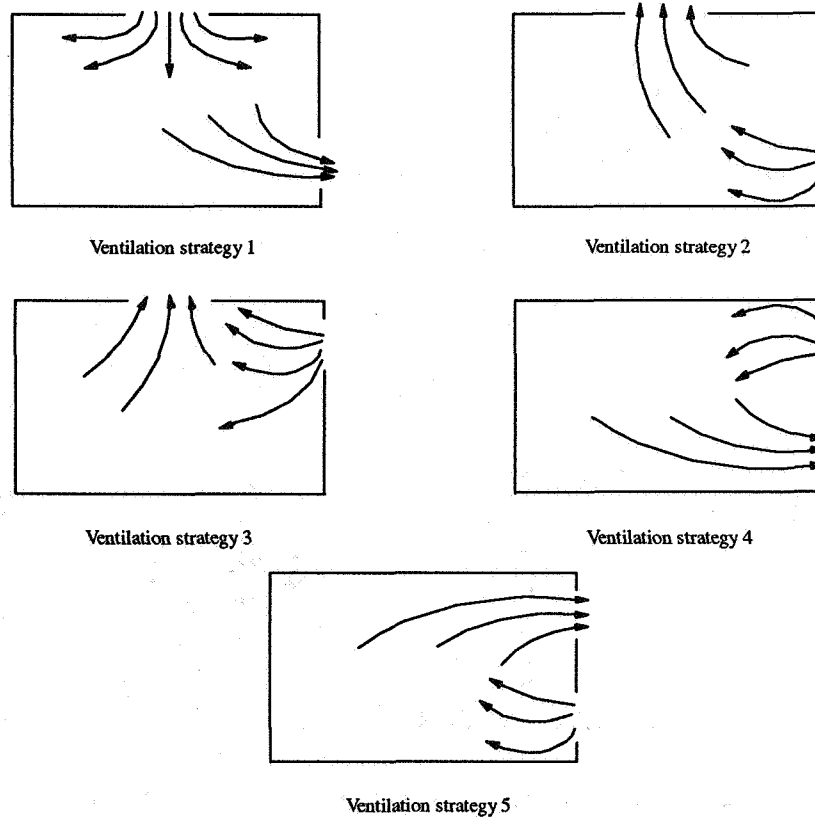


Figure 2 Ventilation strategies for experiment

3. RESULTS AND DISCUSSION

Experimental work was carried out in the chamber to determine average air exchange efficiency for various ventilation strategies using the tracer-gas decay method, defined as:

$$\eta_a = \frac{\tau_{TE}}{\tau_{T1}} \quad (1)$$

and average particle exchange efficiency defined as:

$$\eta_p = \frac{\tau_{PE}}{\tau_{Pp}} \quad (2)$$

Results are given in Table 1. Location D gives the lowest average particle efficiency. Short circuiting may give $\eta_p > 1.0$ for strategies 3, 4 and 5. Strategy 2 gives a higher overall η_p than strategy 1. The particle exchange rates were found to be higher than tracer-gas exchange rates. The difference in tracer-gas and particle exchange rates is due to deposition (or adsorption) of particles on the surfaces of the environmental chamber. This was estimated using the following equation:

$$\alpha = (P - I) \times \frac{V_z}{A} \quad (3)$$

Strategy 1 gives deposition 0.10 - 2.09 $\mu\text{g}/\text{m}^2\text{h}$ only at 17 h^{-1} . Strategy 2 gives deposition 0 - 1.80 $\mu\text{g}/\text{m}^2\text{h}$ for all ventilation rates. Strategy 3 gives deposition 0.09 - 3.69 $\mu\text{g}/\text{m}^2\text{h}$ for 17 - 25.4 h^{-1} . Strategy 4 gives deposition 0 - 4.98 $\mu\text{g}/\text{m}^2\text{h}$ for all ventilation rates. Strategy 5 gives deposition 0 - 1.16 $\mu\text{g}/\text{m}^2\text{h}$ for all ventilation rates.

Strategy	Air change rate, (h ⁻¹)	τ_{PA} (mins) (η_A)	τ_{PB} (mins) (η_B)	τ_{PC} (mins) (η_C)	τ_{PD} (mins) (η_D)	τ_{PE} (mins)	τ_{TA} (mins) (η_A)	τ_{TE} (mins)
1	25.4	3.53 (0.90)	3.34 (0.95)	3.45 (0.92)	3.72 (0.85)	3.18	1.66 (0.91)	1.52
	17	4.46 (0.81)	3.37 (1.07)	3.98 (0.91)	4.98 (0.73)	3.61	2.18 (0.80)	1.74
	14.1	9.68 (0.75)	8.48 (0.85)	9.57 (0.75)	18.15 (0.40)	7.21	3.76 (0.96)	3.61
	7.1	23.90 (0.38)	10.37 (0.86)	11.32 (0.78)	11.92 (0.75)	8.88	5.20 (0.88)	4.55
	4.2	23.40 (0.68)	16.99 (0.93)	21.80 (0.73)	24.02 (0.66)	15.82	11.01 (0.90)	9.88
2	25.4	2.92 (0.84)	3.74 (0.66)	3.55 (0.69)	3.28 (0.75)	2.46	0.74 (1.16)	0.85
	17	4.33 (1.08)	4.74 (0.98)	4.67 (1.00)	5.27 (0.89)	4.67	1.86 (1.07)	1.98
	14.1	4.89 (1.10)	5.00 (1.07)	4.94 (1.08)	5.73 (0.93)	5.35	2.43 (1.01)	2.44
	7.1	10.16 (1.03)	10.39 (1.00)	10.53 (0.99)	11.47 (0.91)	10.42	6.07 (0.98)	5.93
	4.2	69.13 (0.50)	48.05 (0.72)	57.43 (0.60)	59.78 (0.58)	34.51	25.39 (1.00)	25.35
3	25.4	2.33 (1.01)	2.59 (0.91)	2.83 (0.83)	3.01 (0.79)	2.36	0.79 (1.02)	0.81
	17	4.96 (1.03)	4.62 (1.11)	5.23 (0.98)	5.41 (0.95)	5.11	1.53 (1.03)	1.58
	14.1	12.96 (0.86)	11.98 (0.92)	12.23 (0.91)	12.42 (0.89)	11.07	3.61 (0.95)	3.44
	7.1	17.65 (1.00)	15.47 (1.14)	17.18 (1.03)	18.55 (0.95)	17.67	7.96 (2.57)	20.45
	4.2	15.62 (1.12)	18.50 (0.95)	22.38 (0.78)	19.34 (0.90)	17.49	9.11 (1.25)	11.41
4	25.4	2.31 (1.11)	2.73 (0.94)	2.91 (0.88)	3.13 (0.82)	2.56	1.12 (1.00)	1.12
	17	3.72 (0.96)	4.25 (0.84)	4.67 (0.77)	4.63 (0.77)	3.58	1.34 (0.81)	1.09
	14.1	3.79 (0.99)	3.83 (0.98)	4.16 (0.90)	4.47 (0.84)	3.76	1.59 (0.91)	1.45
	7.1	5.92 (1.21)	5.35 (1.34)	5.23 (1.37)	7.98 (0.90)	7.16	3.46 (0.60)	2.06
	4.2	16.05 (0.70)	27.38 (0.41)	22.24 (0.51)	28.94 (0.39)	11.24	12.59 (0.75)	9.39
5	25.4	2.91 (1.17)	4.63 (0.74)	4.92 (0.69)	5.42 (0.63)	3.41	0.92 (0.88)	0.81
	17	4.74 (1.14)	6.29 (0.86)	6.20 (0.87)	7.09 (0.76)	5.41	1.98 (0.83)	1.65
	14.1	6.91 (0.98)	6.77 (1.00)	6.90 (0.98)	7.62 (0.89)	6.77	3.03 (0.97)	2.92
	7.1	12.58 (0.87)	10.59 (1.03)	11.40 (0.96)	11.95 (0.92)	10.95	6.14 (1.19)	7.29
	4.2	35.55 (0.81)	33.15 (0.87)	35.50 (0.81)	37.05 (0.78)	28.71	20.28 (0.96)	19.40

Table 1 Experimental results

4. CFD MODELLING

The CFD code FLUENT was used to simulate three-dimensional, isothermal and non-reacting particle movement in the previously described, ventilated single zone, by solving the Navier-Stokes equations and equations governing the dynamic behaviour of particles. The particle equations, in Lagrangian formulation as shown below, take into account the effect on particle movement of particle inertia, aerodynamic drag and gravitational force:

$$\frac{du_p}{dt} = F_D(u_p - u_\infty) + \frac{g_x(\rho_p - \rho_\infty)}{\rho_p} + F_x \quad (4)$$

$$F_D = \frac{18\mu C_D Re}{\rho_p D_p^2 24} \quad (5)$$

$$Re = \frac{\rho D_p |V_p - V_\infty|}{\mu} \quad (6)$$

$$C_D = a_1 + \frac{a_2}{Re} + \frac{a_3}{Re^2} \quad (7)$$

These are the equations for the x-coordinates in a Cartesian system and those for the other two axes are in similar forms. The 3-D computation domain used in this CFD analysis is shown in Figure 3 and it has the same dimensions, opening positions and opening sizes as discussed in the previous section. The amount of air supplied to the room through the inlet and that extracted via the outlet are both 254m³/h, giving rise to an average flow velocity of 0.14m/s at the openings. Particles are assumed to rebound from solid boundaries with a coefficient of restitution of 1. It is also assumed that the particles are spherical, which is reasonable, considering that the particles used in corresponding experiments are tiny droplets, shaped by the force of surface tension. The density of the oil used for smoke generation and thus that of the particles is 865kg/m³. One thousand particles of identical diameter (2µm) and properties were uniformly distributed in the domain at the beginning of the test and their tracks and time of escape through the outlet were monitored. The number of particles remaining in the domain and thus the average particle concentration at any given moment was recorded. This was then compared with corresponding experimental results to determine the accuracy of the CFD simulation.

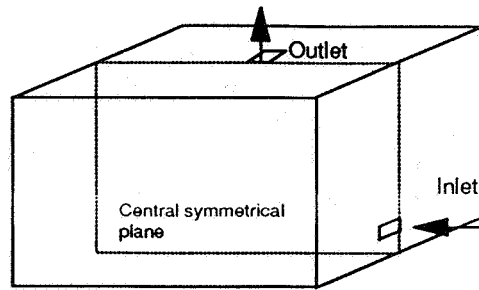


Figure 3 Schematic of building zone used in computation

Figure 4 shows the predicted (squares) and measured (short line sections) particle concentration histories. The normalised concentrations enable direct comparison between the two histories although greatly different number of particles were involved in the prediction and the tests because computing resources impose practical limits on the number of particles that can be traced. Both the predicted and the measured concentrations were assumed to have a relative concentration of unity at 60 seconds. This time lag allows the flow in the test chamber to be reasonably established and stable from 0 second. As can be seen, particle concentrations decreased sharply indicating rapid removal of particles from the test chamber through the outlet by the ventilating flow. In both experiment and simulation, the concentration is close to zero at 20 minutes, although the decrease in the former is slower than that in the latter. This discrepancy is probably due to the rather uncertain boundary conditions, in terms of particle deposition and resuspension, for the test chamber walls. Two particle sizes were used, $2\mu\text{m}$ (the same as that used in the experiments) and $10\mu\text{m}$, but no difference in particle behaviour were observed in the simulation results under the conditions adopted in this study.

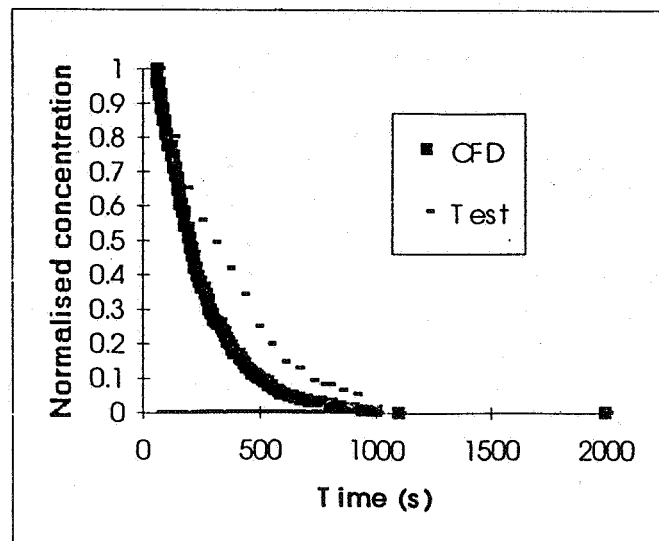


Figure 4 Histories of average particle concentration obtained from CFD and tests

5. CONCLUSIONS

- i) Displacement flow has high values of average particle effectiveness and average air effectiveness compared with other flow strategies used for this study.
- ii) The distribution of particles in the environmental chamber is not uniform, the corner away from the door (Point D) has the lowest age-of-particle.
- iii) CFD simulation of particle movement has been carried out using the CFD code FLUENT. The history of particle concentration was predicted by monitoring 1000 particles uniformly distributed in the computation domain at the beginning of the tracking exercise. Comparison of the predicted history with that obtained from experiments shows reasonable agreement, which could be further improved by adopting more realistic boundary conditions in the CFD simulation.

ACKNOWLEDGEMENTS

The authors wish to thank the financial support of the Engineering and Physical Sciences Research Council (EPSRC).

REFERENCES

1. BERGLUND, B., BRUNEKREEF, B., KNOPPEL, H., LINDVALL, T., MARONI, M., MOLHAVE and SKOV, P.
"Effects of Indoor Air Pollution on Human Health"
Report No. 10, European concerted action "Indoor Air Quality and Its Impact on Man"
1991
2. FARRANCE, K. and WILKINSON, J.
"Dusting Down Suspended Particles"
Building Services 12, 1990, pp45-46.
3. NAZAROFF, W.W. and CASS, G.R.
"Protecting museum collections from soiling due to the deposition of airborne particles"
Atmospheric Environment, Vol 25A, No. 5/6, 1991, pp841-852.